THE JOURNAL OF BIOLOGICAL CHEMISTRY VOL. 284, NO. 51, pp. 35872–35884, December 18, 2009

Abnormal Expression of Collagen IV in Lens Activates Unfolded Protein Response Resulting in Cataract*[S]

Received for publication, August 27, 2009, and in revised form, October 1, 2009 Published, JBC Papers in Press, October 26, 2009, DOI 10.1074/jbc.M109.060384

Zeynep Firtina[‡1], Brian P. Danysh[‡], Xiaoyang Bai[§], Douglas B. Gould[§2], Takehiro Kobayashi[¶], and Melinda K. Duncan[‡3]

From the [‡]Department of Biological Sciences, University of Delaware, Newark, Delaware 19716, the [§]Department of Ophthalmology and Anatomy, Institute of Human Genetics, University of California, San Francisco, California 94143, and the [¶]Department of Homeostatic Regulation and Development, Niigata University Graduate School of Medical and Dental Sciences, 951-8510 Niigata City, Japan

Human diseases caused by mutations in extracellular matrix genes are often associated with an increased risk of cataract and lens capsular rupture. However, the underlying mechanisms of cataract pathogenesis in these conditions are still unknown. Using two different mouse models, we show that the accumulation of collagen chains in the secretory pathway activates the stress signaling pathway termed unfolded protein response (UPR). Transgenic mice expressing ectopic *Col4a3* and *Col4a4* genes in the lens exhibited activation of IRE1, ATF6, and PERK associated with expansion of the endoplasmic reticulum and attenuation of general protein translation. The expression of the transgenes had adverse effects on lens fiber cell differentiation and eventually induced cell death in a group of transgenic fiber cells. In *Col4a1*$^{+/\Delta ex40}$ mutant mice, the accumulation of mutant chains also caused low levels of UPR activation. However, cell death was not induced in mutant lenses, suggesting that low levels of UPR activation are not proapoptotic. Collectively, the results provide *in vivo* evidence for a role of UPR in cataract formation in response to accumulation of terminally unfolded proteins in the endoplasmic reticulum.

The ocular lens is a transparent, cellular structure that refracts light onto the retina, resulting in high resolution vision. Many environmental risk factors and single gene defects are known or hypothesized to result in clouding of the lens, a condition known as cataract. Cataract is the primary cause of blindness worldwide (1, 2), with autosomal dominant congenital cataract being the leading cause of treatable childhood blindness (3, 4). Cataract surgery is the most commonly performed surgical operation in the United States and consumes 60% of the Medicare budget for vision (5, 6).

Cataract can be a multifactorial disease and is often associated with systemic or genetic disorders, such as diabetes and Lowe syndrome (7–9). Notably, human diseases caused by mutations in extracellular matrix (ECM)[4] genes are also often associated with an increased risk of cataract. Stickler and Marshall syndromes are two disorders caused by mutations in the *COL2A1* gene that are associated with the early onset of distinctive cataracts (10, 11). Alport syndrome, caused by mutations in either the *COL4A3, COL4A4*, or *COL4A5* genes, is also associated with lens capsule abnormalities and cataract formation (12–14). Humans carrying mutations in the *COL4A1* locus often exhibit lens abnormalities and cataracts along with porencephaly and sporadic intracerebral hemorrhage (15–19). To date, approximately 13 independent mutations in the mouse *Col4a1* locus and three independent mutations in mouse *Col4a2* locus have been found to cause vacuolar cataract and lens abnormalities in mice (19–21). However, the underlying mechanisms of cataract pathogenesis resulting from these collagen mutations are still unknown.

In other tissues, mutations in genes encoding secretory pathway proteins have been found to cause endoplasmic reticulum (ER) stress and subsequent activation of the unfolded protein response (UPR), a set of evolutionarily conserved signaling pathways activated upon ER stress (22–28). UPR has been implicated in the pathogenesis of many conformational diseases, such as Alzheimer disease, Parkinson disease, and diabetes, and is being investigated in many others (29–33). UPR pathways are activated following accumulation of unfolded proteins in the ER lumen and attempt to relieve the stress by 1) up-regulating the ER folding capacity through increasing the levels of ER-resident molecular chaperones and expansion of the ER, 2) reducing the demand on the ER through attenuation of protein synthesis, and 3) increasing the clearance of unfolded proteins from the ER through up-regulation of ER-associated degradation (24, 34, 35). However, if these mechanisms cannot relieve the stress, the UPR pathway activates apoptosis (36–38). Mammalian UPR is mediated by three ER-resident transmembrane proteins, IRE1, PERK (PKR-like ER kinase), and ATF6, whose combined activation alters transcriptional and translational programs and induces profound changes in cellular processes, such as cell growth, differentiation, and survival (38–40). Notably, UPR pathways are induced in the lens in response

* This work was supported, in whole or in part, by National Institutes of Health, NEI, Grants EY015279 (to M. K. D.) and EY02162 (to D. B. G.). The University of Delaware Core Imaging facility was supported by Idea Networks of Biomedical Research Excellence Program Grant P20 RR16472.

[S] The on-line version of this article (available at http://www.jbc.org) contains supplemental Table 1 and Figs. 1 and 2.

[1] Recipient of a Sigma Xi-NAS grant-in-aid.

[2] Recipient of grants from That Man May See and Research to Prevent Blindness.

[3] To whom correspondence should be addressed. Tel.: 302-831-0533; Fax: 302-831-2281; E-mail: duncanm@udel.edu.

[4] The abbreviations used are: ECM, extracellular matrix; ER, endoplasmic reticulum; UPR, unfolded protein response; RT, reverse transcription; TUNEL, terminal deoxynucleotidyltransferase-mediated dUTP nick end labeling; WT, wild type; eIF2α, eukaryotic initiation factor 2; E*n*, embryonic day *n*; P*n*, postnatal day *n*.

to oxidative stress; however, the relative contributions of UPR and oxidative damage to lens pathogenesis are difficult to ascertain (41, 42).

Here we test the hypothesis that the presence of unfolded proteins within the lens secretory pathway results in UPR activation, disrupts lens differentiation and/or lens cell survival, and contributes to cataract pathogenesis. We first investigated whether the chronic production of unassembled collagen IV α chains in the lens results in ER stress, the activation of UPR pathways, and the cellular changes leading to cataract formation. We then determined that UPR pathways were also activated in the lenses from *Col4a1* mutant mice, suggesting that UPR induction may be generally important in the pathogenesis of cataracts associated with the mutation of ECM genes.

EXPERIMENTAL PROCEDURES

Generation of Transgenic and Mutant Mice—All experiments using transgenic animals were approved by the University of Delaware Institutional Animal Care and Use Committee. The δenαA plasmid containing the hybrid δen/αA-crystallin promoter, the rabbit β-globin intron, and the human growth hormone poly(A) signal was a gift from Lixing Reneker (University of Missouri, Columbia, MO) (43). The mouse cDNAs for *Col4a3* and *Col4a4* were created as described previously (44). After the cDNA for either *Col4a3* or *Col4a4* was placed between the rabbit β-globin intron and human growth hormone poly(A) signal in δenαA, the fragment containing the promoter, cDNA, intron, and poly(A) signal was liberated from the backbone plasmid by restriction enzyme digestion and gel-purified. This fragment was microinjected into the pronuclei of FVB/N fertilized eggs by the University of Delaware transgenic mouse facility as described previously (45). The genotyping of the transgenic mice is described in the supplemental material.

Col4a1$^{+/\Delta ex40}$ mice were bred at the University of California, San Francisco, animal facility and genotyped as previously described (19). All experiments using mutant animals were approved by the University of California Institutional Animal Care and Use Committee.

Embryos used in the study are staged by designating the day that the vaginal plug was observed in the dam as E0.5. Postnatal mice were staged by designating the day of birth as P0.

Morphological Analysis—For gross documentation of alterations in lens structure, lenses were isolated under a dissecting microscope and photographed under dark field optics. For histological analysis, eyes (postnatal mice) or heads (embryos) were isolated and immediately fixed in Pen-Fix (Richard Allan Scientific, Kalamazoo, MI) for 2 h prior to paraffin embedding. Serial 6-μm sections were cut and mounted on slides. Selected slides were then stained by hematoxylin and eosin by standard methods and visualized by a light microscope.

Scanning Electron Microscopy—Scanning electron microscopy was performed as described by Duncan *et al.* with some minor modifications (46). The protocol is described in detail in the supplemental material.

Immunolocalization—All antibodies used in this study are described in the supplemental material.

Immunohistochemistry—Paraffin sections, prepared as above for hematoxylin and eosin, were deparaffinized, incubated with rabbit anti-bovine β-crystallin or rabbit anti-bovine γ-crystallin antibodies (gifts of Samuel Zigler, NEI, National Institutes of Health, Bethesda, MD). Antibody signal was then detected with the horseradish peroxidase Dako Envision kit (Dako Laboratories, Carpinteria, CA).

Immunofluorescence—All immunofluorescence experiments were performed as described previously (47). A detailed protocol is described in the supplemental material.

Western Blotting—Lenses were isolated and immediately homogenized with 0.1 ml of ice-cold lysis buffer (50 mM Tris-HCl, pH 8.0, 150 mM NaCl, 1% Nonidet P-40, 0.5% sodium deoxycholate, 0.1% SDS) supplemented with Halt protease and phosphatase inhibitor mixture (Thermo Scientific, Rockford, IL). The insoluble material was removed by centrifugation at 12,000 × *g* for 30 min. Final protein concentrations were determined using a Bio-Rad protein assay kit according to the manufacturer's specifications. Forty micrograms of total protein was resolved by SDS-polyacrylamide gel and transferred onto supported nitrocellulose membranes (Bio-Rad). The protein blots were blocked with SuperBlock T20 blocking buffer (Thermo Scientific) overnight at 4 °C and incubated with the primary antibody in the same blocking buffer for 2 h. After incubation with secondary antibodies conjugated with horseradish peroxidase (Calbiochem) for 1 h at room temperature, the signals were detected using an ECL detection kit (Amersham Biosciences). The intensity of the signal for collagen IV chains were quantified using Photoshop histogram analysis.

RNA Preparation and RT-PCR—Total RNA from lenses was extracted using the SV total RNA isolation kit (Promega). For RT-PCR, 20 ng of total RNA was used for each reaction. The primers used are Xbp1 Fwd (5′-GAA CCA GGA GTT AAG AAC ACG-3′) and Xbp1 Rev (5′-AGG CAA CAG TGT CAG AGT CC-3′) for Xbp1 splicing and CHOP Fwd (5′-CAC TAC TCT TGA CCC TGC GT-3′) and CHOP Rev (5′-GGA GAG ACA GAC AGG AGG TGA-3′) for CHOP expression.

TUNEL Assay—Sections were prepared in the same way as in immunofluorescence studies. Frozen sections were then fixed in ice cold 1:1 acetone-methanol for 20 min, washed in 1× phosphate-buffered saline, and blocked for 20 min in equilibration buffer containing 1× TE (10 mM Tris, 1 mM EDTA, pH 8.0), 1× terminal transferase buffer, and 1.67 mM $CoCl_2$ at room temperature (Roche Applied Science). Then excess equilibration buffer was absorbed with a KimWipe, and reaction buffer containing 0.005 mM ChromaTide Alexa Fluor 488-5-dUTP (Molecular Probes, Inc., Eugene, OR), 0.01 mM dATP (both diluted in equilibration buffer), and 1 μl of TdT enzyme (Roche Applied Science) was added onto the sections and incubated at 37 °C for 60–90 min. Sections without TdT enzyme were used as negative controls. Slides were soaked in 1× SSC for 15 min at room temperature to stop the reaction, washed in 1× phosphate-buffered saline, and stained with Draq5 diluted 1:2000 in 1× phosphate-buffered saline for 5 min. Slides were rinsed briefly in phosphate-buffered saline, mounted, and visualized using a Zeiss LSM 510 confocal microscope (Carl Zeiss Inc., Göttingen, Germany).

Protein Translation Assay—Lenses were isolated and immediately placed in a 6-well dish with Medium 199 (Mediatech Inc., Manassas, VA) supplemented with a tritium (^{3}H)-labeled

amino acid mixture (catalog number ART0328, American Radiolabeled Chemicals Inc., St. Louis, MO) to a final concentration of 20 μCi/ml. Lenses were incubated for at least 6 h in a humidified atmosphere of 5% CO_2 and 95% air at 37 °C, as described previously (48). Medium was removed, and lenses were washed three times with non-radioactive Medium 199. Thirty microliters of lysis buffer (50 mM Tris-HCl, pH 8.0, 150 mM NaCl, 1% Nonidet P-40, 0.5% sodium deoxycholate, 0.1% SDS) supplemented with halt protease and phosphatase inhibitor mixture (Thermo Scientific) was added, and lenses were lysed using a mortar and pestle. The radioactivity incorporated into the lenses were determined as previously described (49). Briefly, 10 μl of the cell lysate was spotted on a Whatman glass microfiber filter (catalog number 1822 021). The filter then was washed with boiling trichloroacetic acid for 5 min and twice more with cold trichloroacetic acid (5 min each). The filter was rinsed briefly in ice-cold 95% ethanol and then in ice-cold acetone and air-dried. The radioactivity remaining on the dried filter was measured with a liquid scintillation counter. To calculate the radioactivity per cubic millimeter volume, the radii of the lenses were determined from lens photographs using Image J, and the lens volume was estimated using the formula, $4/3 \cdot \pi \cdot r^3$. Student's *t* test was performed for statistical analysis.

RESULTS

Overexpression of Col4a3 or Col4a4 in the Embryonic Lens Results in Microphthalmia and Cataract—All six known *Col4* genes, (*a1–a6*), are expressed in the adult mouse lens; however, *Col4a3* and *Col4a4* are not expressed in the embryonic lens, resulting in the absence of the COL4(A3.A4.A5):(A3.A4.A5) heterotrimeric network from the lens capsule until 2–3 weeks postnatal (50). Because the assembly of the COL4(A3.A4.A5) protomer requires the presence of all three subunits, we hypothesized that ectopic expression of either normal *Col4a3* or *Col4a4* alone in the embryonic lens will result in the retention of unassembled single COL4A3 or COL4A4 chains in lens cells inducing the unfolded protein response. Thus, we generated transgenic mice ectopically expressing either *Col4a3* or *Col4a4* in all lens cells starting at the late lens pit stage (E11–E11.5) using the δen/αA-crystallin hybrid promoter (Fig. 1*A*). Two independent founder transgenic mice were derived from each transgene. Both Col4a4 lines (A4-501 and A4-520) and one of the Col4a3 lines (A3-21) had affected lenses, whereas the remaining Col4a3 line, A3-9, had clear lenses (data not shown). The affected transgenic lenses exhibit variable phenotype in lens size and transparency; however, lenses from all three affected lines were significantly smaller and had obvious opacities compared with the normal lens (Fig. 1*B*).

Transgenic Lenses Produce High Levels of Exogenous Collagen Chains That Accumulate in Lens Fiber Cells—To determine when the expression of the transgenes starts, we used antibodies specific to COL4A3 and COL4A4 chains. Both lines did not have detectable transgene expression up to E12.5 (data not shown). At E12.5, we detected high expression of the *Col4a3* transgene in A3-21 lens fiber cells (Fig. 2*A*, *top*), whereas the A3-9 line, which has clear lenses, did not have detectable *Col4a3* expression (Fig. 2*A*, *bottom*), suggesting a correlation between the cataract phenotype and the expression of the

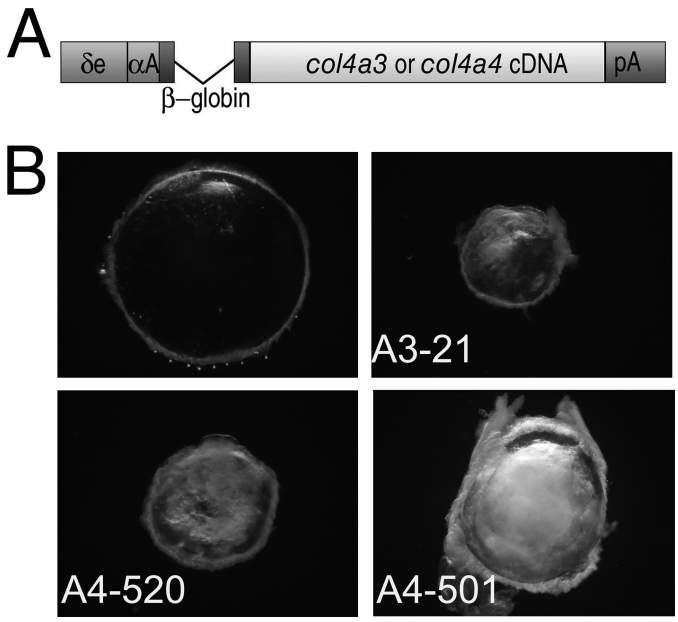

FIGURE 1. **The ectopic expression of *Col4a3* or *Col4a4* transgenes in the embryonic mouse lens results in lens opacity and microphthalmia.** *A*, diagram of the transgene vector. The chick δ1-crystallin enhancer (*δen*) fused to a mouse short αA-crystallin promoter (*αA*) was used to drive the expression (43). The cDNAs for the transgenes were placed between the rabbit *β*-globin intron (640 bp) and the human growth hormone poly(A) signal (*pA*; 660 bp). *B*, dark field images of the 2.5 months old WT and transgenic lenses. Both Col4a4 lines (*bottom*) and one of the Col4a3 lines (*top right*) had significantly smaller eyes with obvious opacities and other lens defects. *A4-520* and *A4-501*, two Col4a4 lines; *A3-21*, Col4a3 line.

transgene. When overexposed, a slight amount of COL4A3 was also detected around the lens, suggesting the secretion of a small amount of the transgene product (Fig. 2*A*, *middle*). Similarly, in the affected A4-520 line, we detected prominent expression of the *Col4a4* transgene in lens fiber cells starting from E12.5 (Fig. 2*B*, *top*), whereas there was no detectable *Col4a4* expression in the WT lens at this age (Fig. 2*B*, *bottom*). When overexposed, a weak fluorescent signal was also detected around the lens, suggesting the secretion of some of the transgene (Fig. 2*B*, *middle*). By Western blotting using a pan-collagen IV antibody, we confirmed that the affected transgenic lines (A4-520 and A3-21) have higher levels of soluble collagen IV chains in the lens at E14.5 (Fig. 2*C*). Quantification of the signal on the membrane suggested that the increase in soluble collagen IV chains is ~35% for the A3-520 line and 48% for the A3-21 line. Notably, we did not detect abnormal expression of *Col4a4* in the *Col4a3*-overexpressing A3-21 line or *vice versa*, suggesting that the overexpression of one chain does not cause abnormal expression of the other (data not shown). These results suggested that the overexpressed collagen chains were unable to exit the ER and instead accumulate within lens fiber cells.

Lenses Overexpressing Collagen IV Chains Have Defective Fiber Cells—We then analyzed how the intracellular accumulation of collagen IV interferes with lens development and differentiation. Most of the lens is composed of concentric layers of elongated fiber cells that are formed by the continuous differentiation of epithelial cells at the lens equator. Because there is no turnover of lens fiber cells, the steady addition of new fiber cells throughout life concentrates the older fibers in the center

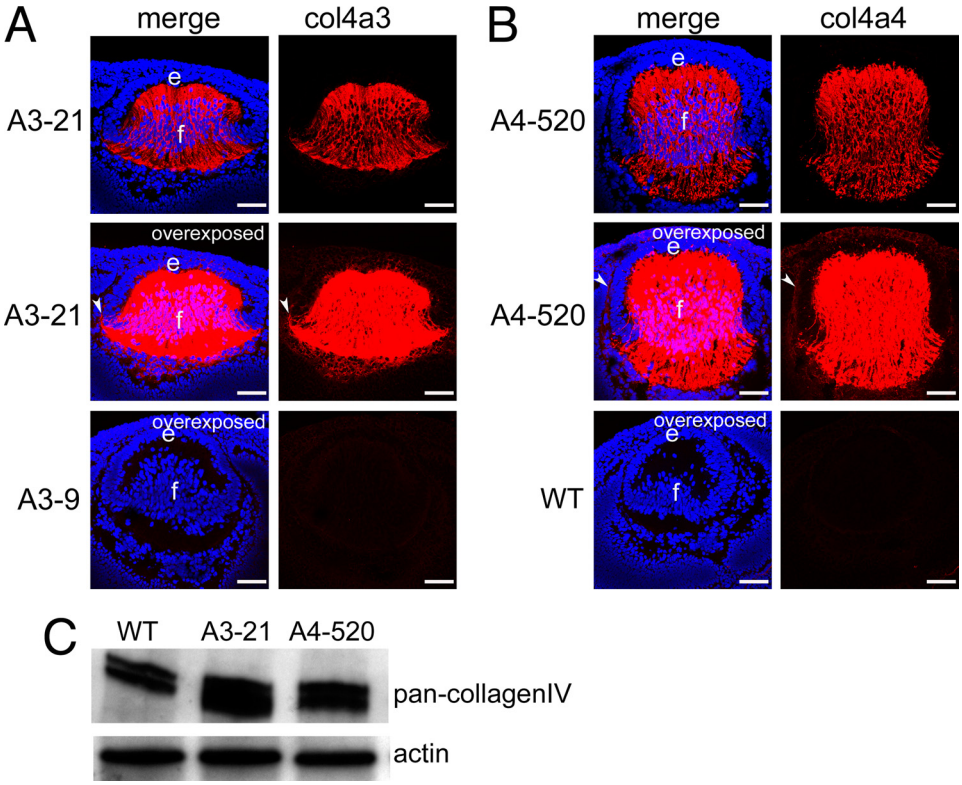

FIGURE 2. **Exogenous COL4A3 or COL4A4 chains accumulate to high levels in affected transgenic fiber cells.** *A*, a chain-specific antibody against COL4A3 was used to detect the expression in the affected A3-21 (*top* and *middle*) and the unaffected A3-9 (*bottom*) lenses. At E12.5, *Col4a3* transgene is highly expressed in the affected A3-21 fiber cells, whereas there is no detectable expression in the unaffected A3-9 lenses at this age. *B*, a chain-specific antibody against COL4A4 was used to detect its expression in the affected A4-520 (*top* and *middle*) and the WT (*bottom*) lenses. At E12.5, *Col4a4* transgene is highly expressed in the affected A4-520 fiber cells, whereas there is no detectable expression in the wild type lenses at this age. The gain for the *middle* and *bottom panels* in both *A* and *B* was increased ~25% to obtain an overexposed image showing possible secretion of exogenous collagen chains. The *arrowheads* indicate the detection of secreted collagen chains around the lens. *Bars*, 77 μm; *e*, epithelium; *f*, fiber cells. *Red*, collagen IV chain; *blue*, DNA. *C*, expression of collagen IV chains in E14.5 lenses was detected by Western blotting using a pan-collagen IV antibody. The affected A4-520 and A3-21 lenses have elevated levels of soluble collagen IV chains.

of the lens (51, 52). We analyzed transgenic embryonic lenses using hematoxylin and eosin staining starting from E11.5. In both transgenic lines, primary fiber cell differentiation occurred normally as in WT lenses (data not shown), and elongating transgenic fiber cells reached to the epithelium (Fig. 3, *B* and *C*). However, by E15.5, A3-21 fiber cells lost contact with the epithelium, resulting in the formation of a gap between the epithelium and fiber cells (Fig. 3*F*). Similarly, by E16.5, A4-520 fiber cells detached from the epithelium (Fig. 3*H*). This phenotype suggested that transgenic lenses have a fiber cell elongation defect, where the fiber cells expressing the transgene cannot keep up with the growing lens. In lenses from newborn mice, the gap between epithelium and fiber cells is mostly closed, suggesting that the elongation defect is partially relieved; however, fiber cells still look abnormal and form a disorganized central mass surrounded by the secondary fibers (Fig. 3, *K* and *L*). A closer examination of the adult transgenic fiber cells by scanning electron microscopy revealed that these fiber cells are irregularly shaped and poorly aligned (Fig. 4, *bottom left*) compared with the uniform hexagonal cells of the normal lens (Fig. 4, *top left*). Also, although normal fiber cells have regularly arrayed ball-and-socket-like lateral membrane interdigitations (Fig. 4, *top right*), transgenic fiber cells have an abnormal lateral membrane structure, resulting in the distortion of the tightly packed fiber cell array (Fig. 4, *bottom right*). Differentiating transgenic fiber cells also retain their nuclei and are strongly stained by the lectin concanavalin A, which binds to carbohydrate moieties in the ER (53, 54), and prohibitin, a marker of the inner mitochondrial membrane, suggesting that the degradation of nuclei and organelles that occurs during normal lens fiber cell differentiation is arrested (supplemental Fig. 1). These results showed that the accumulation of the transgene-derived proteins in lens fiber cells interferes with fiber cell elongation during early embryogenesis and results in altered fiber cell structure and differentiation.

Trangenic Lenses Do Not Have a Major Defect in General Secretion—Next, we tested whether the lens defects seen in transgenic lenses resulted from a general secretion defect caused by the accumulation of high levels of exogenous collagen chains in the secretory pathway. Immunostainings for pan-laminin (data not shown) and the endogenous collagen α chains (A1, A2, A5, and A6) showed that they are secreted normally, forming a capsule around the lens (Fig. 5). Thus, we concluded that the transgenic lenses are not suffering a major global defect in the secretory pathway, suggesting that the pathogenesis in these lenses is mostly due to the presence of unfolded proteins in the secretory pathway.

The Accumulation of Transgenes in the Lens Causes Immunoglobulin-binding Protein (BiP) Up-regulation and Extension of the Endoplasmic Reticulum—One known cellular consequence of protein accumulation in the secretory pathway is the activation of the unfolded protein response. UPR activation changes both transcriptional and translational programs and can have a major effect on cell biology (34, 55, 56). BiP is a major chaperone found in the ER, and its up-regulation has been used as a sensitive indicator of UPR activation (57, 58). BiP immunostaining showed that the affected A4-520 and A3-21 lines have drastically elevated levels of BiP expression at postnatal day 2 (Fig. 6*A*). This BiP up-regulation starts at E12.5 and coincides with the accumulation of collagen chains in lens fiber cells (Fig. 6*B*). Western blot analysis confirmed the increase in BiP protein levels at E14.5 and E16.5 transgenic lenses (Fig. 6*C*). One of the hallmarks of UPR is the activation of factors that induce ER membrane production, resulting in ER expansion (59–62). Transgenic fiber cells do have strong concanavalin A label-

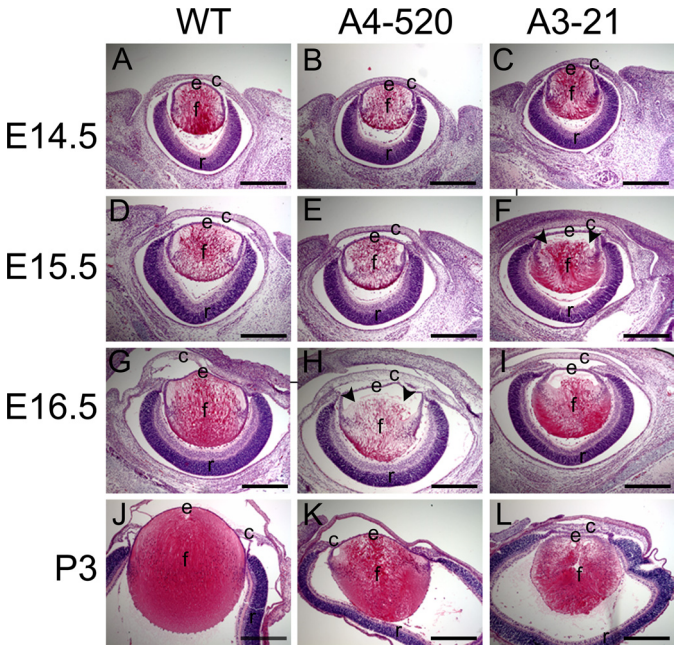

FIGURE 3. **Lens histology was compared between WT (*A*, *D*, *G*, and *J*), A4-520 (*B*, *E*, *H*, and *K*), and A3-21 (*C*, *F*, *I*, and *L*) lenses at different developmental stages.** At E14.5, A4-520 (*B*) and A3-21 (*C*) fiber cells are in contact the epithelium as in WT lenses (*A*). At E15.5, line A3-21 (*F*) fiber cells lose contact with the epithelium, whereas WT (*D*) and A4-520 (*E*) fibers look normal. At E16.5, A4-520 (*H*) fiber cells also lose contact with the epithelium, whereas WT (*G*) fibers grow normally. After birth, A4-520 (*K*) and A3-21 (*L*) lenses were significantly smaller with major lens defects. The *arrowheads* indicate the apical tips of improperly elongated fiber cells. *Scale bar*, 330 μm; *c*, cornea; *e*, epithelium; *f*, fiber cells; *r*, retina. *Pink*, cytoplasm; *purple*, cell nuclei.

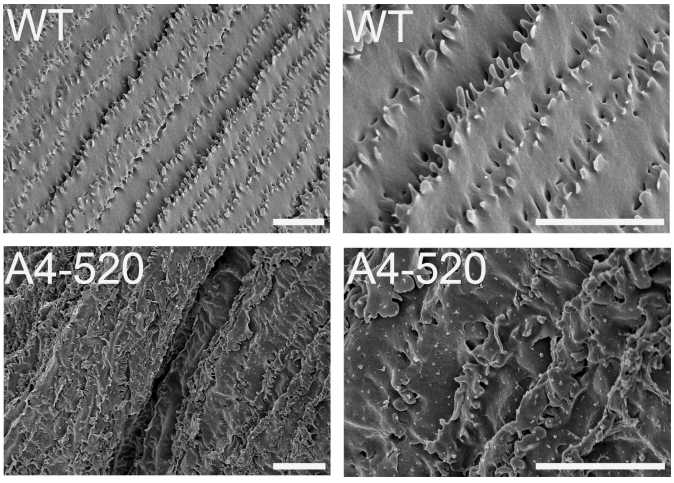

FIGURE 4. **Scanning electron microscopy analysis of the WT and A4-520 fiber cells.** Fiber cells from transgenic mice (*bottom*) are disorganized with irregular interlocking junctions as compared with the regular organization of the WT lens fiber cells (*top*). *Scale bar*, 10 μm.

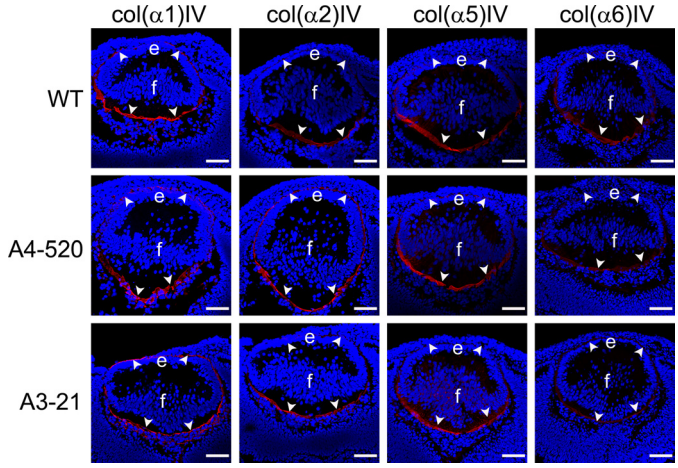

FIGURE 5. **Secretion of COL4A1, -A2, -A5, and -A6 chains is not affected in the transgenic fiber cells.** Chain-specific antibodies against COL4A1, -A2, -A5, and -A6 were used to detect their expression in WT (*top*), A4-520 (*middle*), and A3-21 (*bottom*) lenses. The *arrowheads* indicate the secreted collagen IV chains incorporated into the lens capsule. *Bars*, 77 μm; *e*, epithelium; *f*, fiber cells. *Blue*, DNA; *red*, collagen IV chain.

ing around the nuclei of lens fiber cells and throughout the cytoplasm, suggesting that the ER in transgenic fiber cells has been expanded (Fig. 6*D*). Because these results suggested that the transgenic lenses are experiencing the unfolded protein response, we proceeded to identify which pathways are activated.

The IRE1/Xbp1 Pathway Is Activated in the Transgenic Lenses—The UPR pathway that has been conserved from yeast to mammals is transduced by IRE1 (inositol-requiring enzyme 1), an atypical type I transmembrane protein consisting of an ER luminal dimerization domain as well as cytosolic kinase and endoribonuclease domains (63). Activated IRE1 removes a 26-base intron from the *Xbp1* mRNA, introducing a frameshift and an alternative C terminus to create a potent transcription factor (64–66). Immunostaining using an XBP1 antibody that detects both spliced and unspliced forms of the XBP1 showed that total levels of XBP1 protein start to increase in transgenic lenses by E12.5 (Fig. 7*A*). By RT-PCR analysis using primers designed to differentiate between spliced and unspliced forms, we also detected a relative increase in spliced *Xbp1* mRNA compared with unspliced in the affected transgenic lenses starting from E12.5 (Fig. 7*B*). Furthermore, Western blot analysis demonstrated that the protein generated from the spliced *Xbp1* mRNA (54 kDa) is only found in the transgenic lenses, whereas protein generated from unspliced *Xbp1* mRNA (33 kDa) is found in both WT and transgenics, indicating the ER stress-induced production of the XBP1 transcription factor (Fig. 7*C*). Notably, control lenses also start up-regulating XBP1(U) protein between E14.5 and E16.5. Although unspliced Xbp1 has been shown to bind and regulate spliced Xbp1 function (67), other functions of this protein are still unclear, and its role in normal lens development and differentiation needs to be investigated.

ATF6 Pathway Is Activated in the Transgenic Lenses—Another sensor activated in mammalian UPR is ATF6 (activating transcription factor 6), which, upon ER stress, progresses to the Golgi, where it is cleaved by S1P and S2P proteases, liberating its cytosolic domain as a soluble transcription factor (68–70). There are two ATF6 genes in mammals, *ATF6α* and *ATF6β*, that appear to be regulated by the same mechanism. The staining of lenses with an ATF6α/β antibody, which detects both intact and cleaved (nuclear) forms, showed that total ATF6α/β greatly increases in transgenic lens fiber cells by E12.5 (Fig. 8*A*). By Western blotting, we showed that at E14.5, pro-ATF6α/β is cleaved into a ~50-kDa protein in transgenic lenses, suggesting its activation (Fig. 8*B*). Notably, pro-ATF6α/β was detected as a

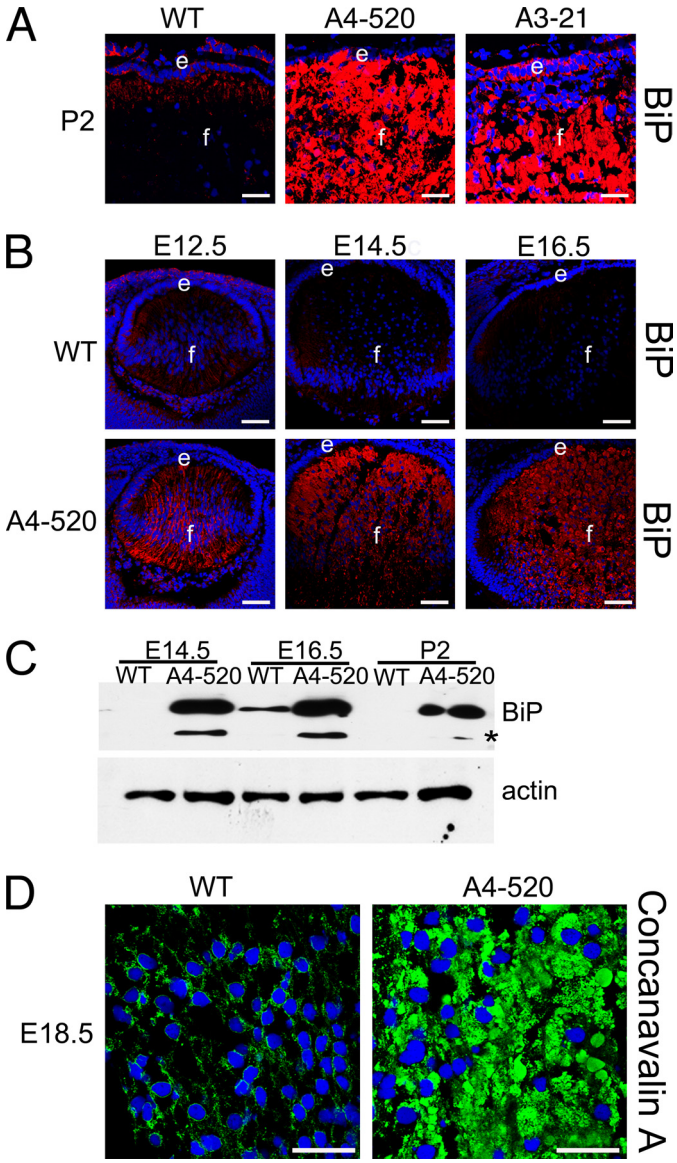

FIGURE 6. **The endoplasmic reticulum in affected transgenic lenses is greatly extended with an up-regulation of the major ER chaperone BiP.** *A*, the expression of BiP (*red*) in 2-day-old WT (*left*), A4-520 (*middle*), and A3-21 (*right*) lenses detected by immunofluorescence. The two affected transgenic lines (A4-520 and A3-21) show much higher levels of BiP expression in lens fiber cells compared with WT lens. *B*, the expression of BiP (*red*) in WT (*top*) and A4-520 (*bottom*) lenses detected by immunofluorescence. In the A4-520 lens, BiP expression starts to up-regulate at E12.5. *Bars*, 77 μm; *e*, epithelium; *f*, fiber cells. *C*, the expression of BiP in WT and A4-520 lenses detected by Western blotting. BiP protein is found at higher levels in E14.5 transgenic lenses and remains elevated after birth. The *asterisks* indicate the smaller 72 kDa band detected by BiP antibody. This band was previously proposed to be a degradation product of wild type BiP (95). WT lenses also express two BiP bands upon longer exposure (not shown). *D*, endoplasmic reticulum was probed in WT (*left*) and A4-520 (*right*) lenses using concanavalin A (*green*). Note that the affected A4-520 fiber cells have much higher staining around the nuclei and throughout the cytoplasm. *Bars*, 40 μm; *e*, epithelium; *f*, fiber cells. In all *panels*, *blue* labels DNA.

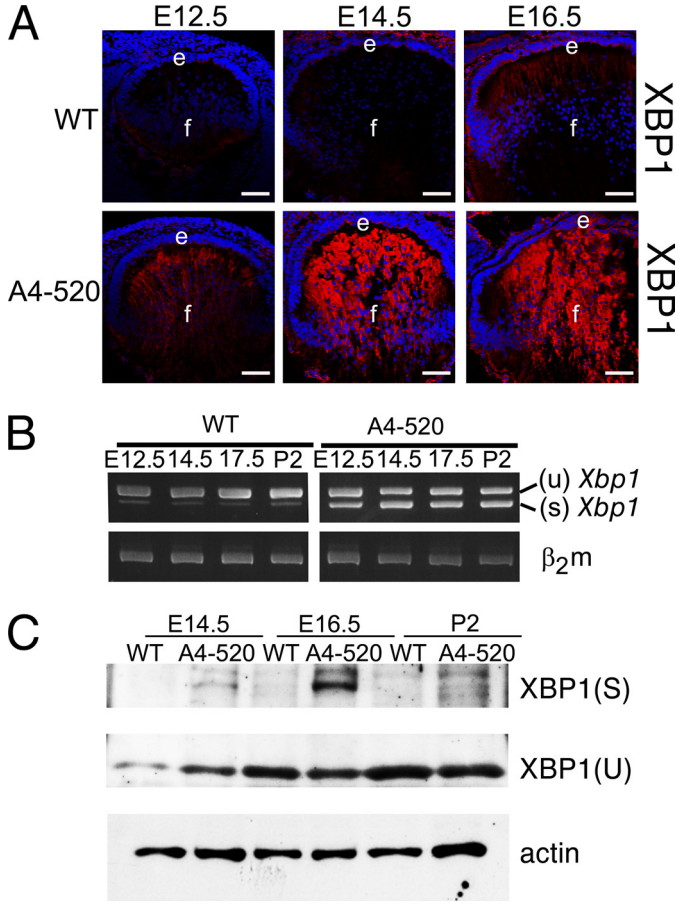

FIGURE 7. **The IRE1/Xbp1 pathway is activated in transgenic lenses.** *A*, expression of XBP1 (both spliced and unspliced) in WT (*top*) and A4-520 (*bottom*) lenses detected by immunofluorescence. The level of XBP1 expression in the A4-520 lens is up-regulated at E12.5 and increases in time. *Bars*, 77 μm; *e*, epithelium; *f*, fiber cells. *Blue*, DNA; *red*, XBP1. *B*, RT-PCR analysis of *Xbp1* splicing. The spliced *Xbp1* mRNA is detected in A4-520 lenses starting at E12.5. β2-Microglobulin was used as a control. *C*, immunoblot analysis of XBP1 protein in WT and A4-520 lenses. Note that the protein produced from spliced *Xbp1* is only found in the affected A4-520 lens, whereas protein from unspliced *Xbp1* is produced both in WT and A4-520 lenses. Actin was used as a loading control.

doublet, which possibly corresponded to fully glycosylated and partially glycosylated forms of ATF6α/β that have previously been shown to arise upon UPR induction (71). Interestingly, at E16.5, both transgenic and normal lenses had cleaved (nuclear) ATF6α/β as the major form, suggesting that ATF6 is also being activated during normal lens development and differentiation between E14.5 and E16.5 (Fig. 8*B*).

PERK Pathway Is Activated in the Transgenic Lenses—The third UPR pathway is induced by PERK, an ER transmembrane protein, whose luminal domain senses ER stress and cytoplasmic domain directly phosphorylates eukaryotic initiation factor 2 (eIF2α) on serine 51, leading to its inactivation. This results in the inhibition of translational initiation for most cellular mRNAs (72–74). We used an antibody specific to phosphorylated PERK to detect active PERK expression. Interestingly, phospho-PERK was also present in the apical tips of normal fiber cells (Fig. 9*A*, *top*); however, its levels were increased at the transgenic fiber cell tips that lost contact with the epithelium (Fig. 9*A*, *bottom*). Immunostaining using an antibody specific to phosphorylated eIF2α showed that there is an increase in the amount of phosphorylated eIF2α in the transgenic fiber cells (Fig. 9*B*). By Western blotting, we confirmed the increase in phosphorylated eIF2α levels in transgenic lenses starting from E14.5, whereas total eIF2α levels are constant, suggesting the possibility of a global translational attenuation in the transgenic lenses (Fig. 9*C*). Notably, in control lenses, total eIF2α levels

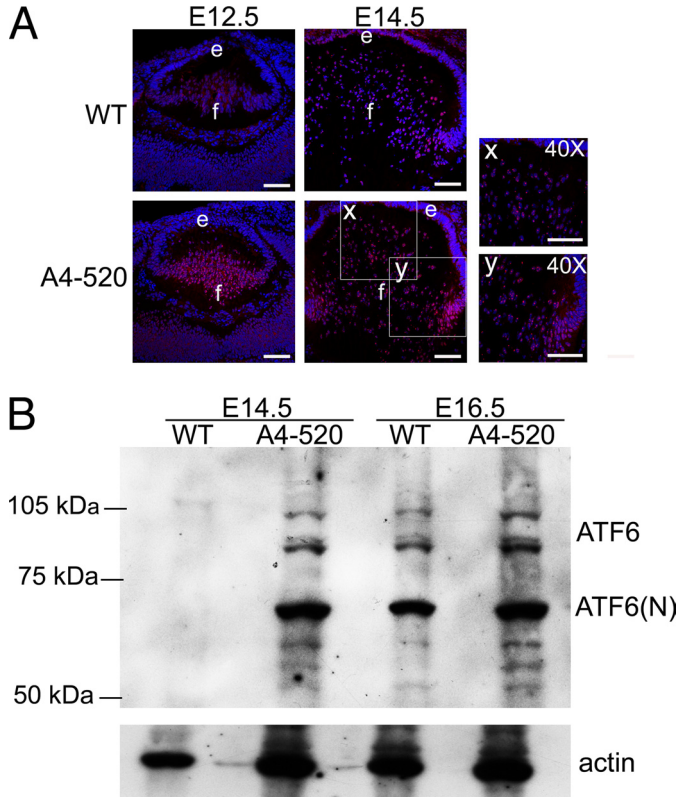

FIGURE 8. **ATF6 pathway is activated in transgenic lenses.** *A*, expression of ATF6 in WT (*top*) and A4-520 (*bottom*) lenses detected by immunofluorescence. Note that the level of ATF6 expression in the A4-520 lens is up-regulated at E12.5 and remains elevated. The ×40 magnification images (*40*×) (*x* and *y*) on the *right* show the *boxed regions* from transgenic lenses. *Bars*, 77 μm; *e*, epithelium; *f*, fiber cells. *Blue*, DNA; *red*, ATF6. *B*, immunoblot analysis of ATF6 protein in WT and A4-520 lenses. Note that at E14.5, ATF6 protein is not detectable in WT lenses, but both forms (full-length/ER-resident and cleaved/nuclear) of ATF6 are highly expressed in A4-520 lenses. Actin was used as a loading control. *ATF6(N)*, nuclear/cleaved form of ATF6.

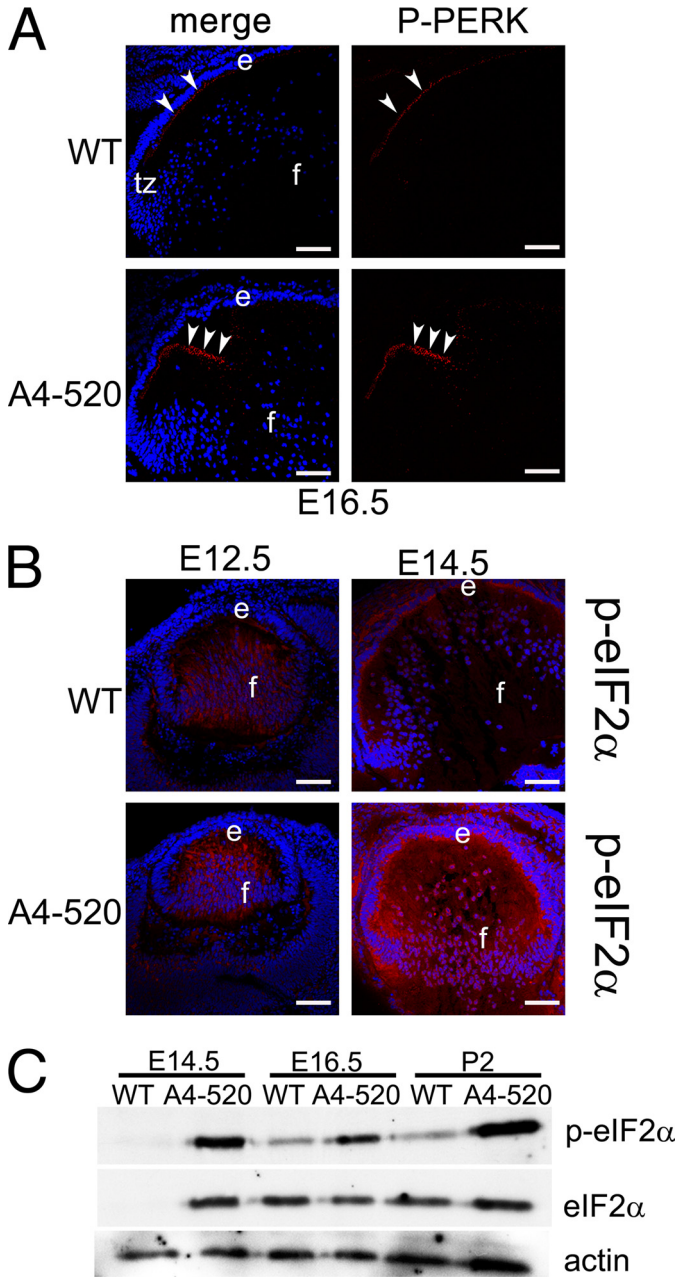

FIGURE 9. **PERK/eIF2α pathway is activated in transgenic lenses.** *A*, expression of phospho-PERK (*red*) in WT (*top*) and A4-520 (*bottom*) lenses detected by immunofluorescence. Note that phospho-PERK levels are increased at the apical tips of A4-520 transgenic fiber cells at E16.5. The *arrowheads* indicate the phospho-PERK detected at the apical tips of normal fiber cells (*top*) and transgenic fiber cells that lost contact with the epithelium (*bottom*). *B*, expression of phospho-eIF2α (*red*) in WT (*top*) and A4-520 (*bottom*) lenses detected by immunofluorescence. Note that phospho-eIF2α levels are initially up-regulated in A4-520 lenses at E12.5 and continue to increase with time. *Bars*, 77 μm; *e*, epithelium; *f*, fiber cells. In all *panels*, *blue* labels DNA. *C*, immunoblot analysis of eIF2α protein in WT and A4-520 lenses. Note that at E14.5, both total and phospho-eIF2α are not detectable in the WT lens, but they are present at high levels in A4-520 lenses. Also note that total eIF2α levels are similar in WT and A4-520 lenses at E16.5 and P2, whereas phospho-eIF2α levels are elevated in the A4-520 lens. Actin was used as a loading control.

also start increasing between E14.5 and E16.5, with a slight increase in phospho-eIF2α levels.

Attenuation of protein translation could have a dramatic effect on lens fiber cell differentiation because one of the characteristics of epithelial to fiber cell differentiation is elevated levels of protein synthesis (75, 76). Particularly, fiber cells synthesize proteins called crystallins, which make up about 90% of the soluble protein content of lens fibers, generating the high refractive index needed for lens transparency and function (77, 78). Immunostaining with pan-β- and γ-crystallin antibodies indicated that their expression is decreased in the transgenic lenses at E16.5 (Fig. 10*A*). When we compared BiP, γ-crystallin, and actin levels in 1% of lens soluble proteins between normal and transgenic lenses by Western blotting, BiP levels were much higher, and γ-crystallin levels were reduced in transgenic lenses, whereas actin levels were similar between the two samples, confirming the apparent decrease in γ-crystallin levels seen by immunohistochemistry (Fig. 10*B*). In order to test whether the decrease in crystallin synthesis is due to a global defect in protein translation, we measured the protein translation rate in intact lenses by incubating freshly isolated E17.5 lenses in cell culture medium supplemented with a tritium-labeled amino acid mixture. When we compared the amount of radioactivity incorporated in newly synthesized proteins within the same lens volume, transgenic lenses incorporated significantly less radioactivity in newly synthesized proteins over the course of the incubation. This indicated that transgenic lenses had a reduced protein translation rate (Fig. 10*C*).

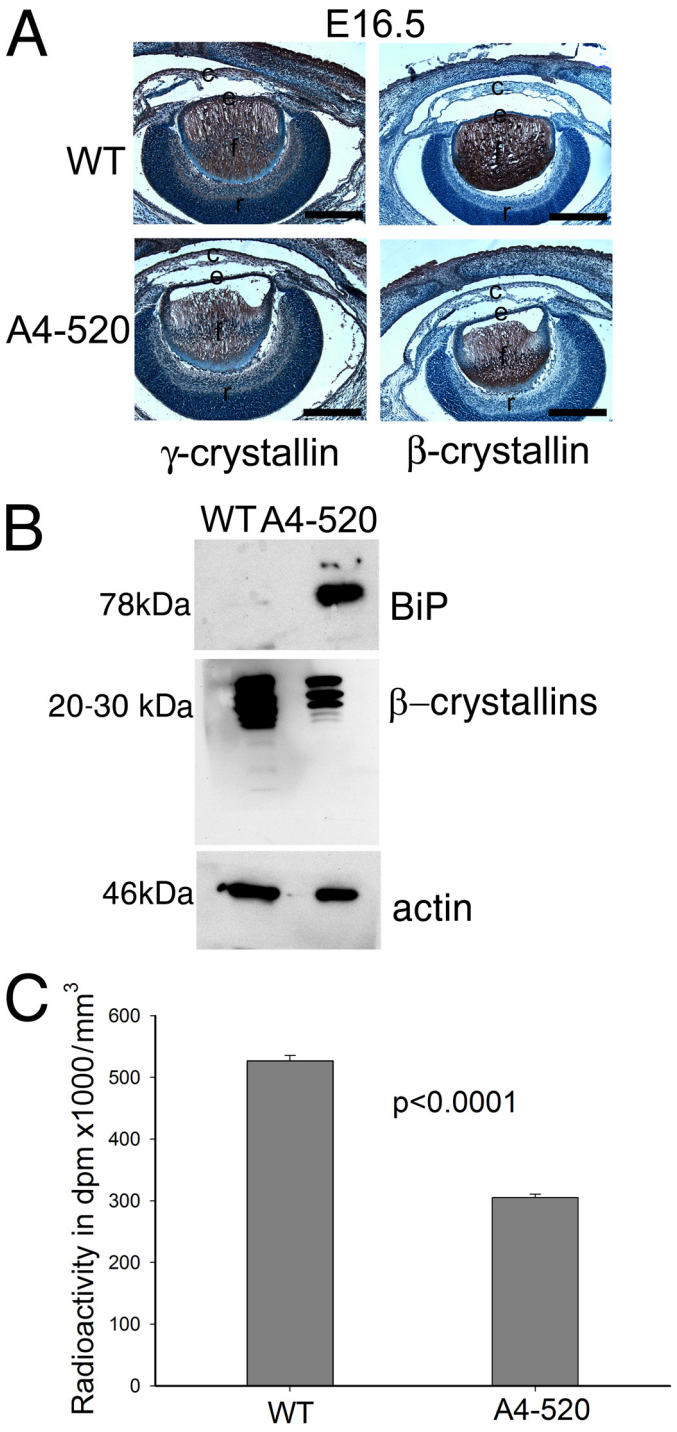

FIGURE 10. **Protein Translation is inhibited in the transgenic lenses.** *A*, expression of γ (*left*) and β crystallins (*right*) in WT (*top*) and A4-520 lenses (*bottom*) detected by immunohistochemistry. At E16.5, A4-520 lenses have less crystallin expression as compared with WT lenses. *Bars*, 330 μm. *c*, cornea; *e*, epithelium; *f*, fiber cells; *r*, retina. *Blue*, DNA; *brown*, crystallins. *B*, 1% of lens soluble proteins were subjected to SDS-PAGE, and the expression of BiP, β-crystallins, and actin was detected by immunoblotting. In 1% of lens soluble proteins, compared with WT lenses, A4-520 lenses have much higher levels of BiP protein and lower levels of β-crystallins, whereas actin levels are similar. *C*, protein translation rate was measured in WT and A4-520 lenses by incubating freshly isolated E17.5 lenses in Medium 199 supplemented with ^{3}H-labeled amino acid mixture. The *y* axis shows the radioactivity measured in dpm/ml^3 of lens volume. The *bars* represent the average radioactivity measured in WT and A4-520 lenses. Statistical analysis was done using Student's *t* test. $p < 0.0001$.

PERK-mediated phosphorylation of eIF2α also results in the enhanced translation of ATF4, a b-ZIP transcription factor of the cyclic AMP-response element-binding protein family (79, 80). We detected intense cytoplasmic ATF4 staining in both normal and transgenic fiber cells at E12.5 (Fig. 11*A*, *top*); however, this expression was greatly reduced at E14.5 lenses (Fig. 11*A*, *bottom*). Although the cytoplasmic expression was reduced, in transgenic lenses, ATF4 continued to be expressed by a group of fiber cells and became strongly nuclear, suggesting its involvement in transcriptional activation of UPR-responsive genes (Fig. 11*A*, *bottom right*). By Western blotting using an ATF4 antibody, we detected two major bands. The lower band existed in both normal and transgenic lenses, whereas the 50 kDa band was only present in the transgenic lenses (Fig. 11*B*). This 50-kDa ATF4 has been previously reported to be induced in a variety of cancer cells upon hypoxia (81). An important UPR-specific target gene of ATF4 is *CHOP/GADD153*, a b-ZIP transcription factor highly up-regulated during UPR (82, 83). By RT-PCR, we found that *Chop* transcript levels are increased in transgenic lenses starting from E14.5 (supplemental Fig. 2). By immunostaining, we detected strong nuclear CHOP expression in some of the transgenic fiber cells starting from E14.5, whereas there was no CHOP expression in the normal lenses (Fig. 11*C*). By Western blotting using an antibody against CHOP, we detected two major bands between 25 and 30 kDa, whereas CHOP is reported to be a 29-kDA protein. The larger band was only found in transgenic lenses, indicating the UPR-specific production of the CHOP transcription factor (Fig. 11*B*). Although another possible outcome of the activated PERK pathway is autophagy (84), we found no evidence of this by looking at the conversion of LC3 by Western blotting and immunostaining (data not shown).

Apoptosis Is Induced in the E18.5 Transgenic Lenses—Because chronic or severe UPR activation can initiate apoptosis, we investigated whether there is increased cell death in the transgenic lenses. Immunostaining of lenses with an antibody specific for the cleaved form of caspase 3 did not reveal any apparent apoptotic cells prior to E18.5. However, at E18.5, a few central fiber cells of transgenic lenses positively stained for cleaved caspase 3 (Fig. 12, *A* and *B*). We also detected TUNEL-positive central fiber cells in E18.5 transgenic lenses (Fig. 12, *E* and *F*), whereas there were no TUNEL-positive cells in normal lens sections at this age (Fig. 12, *C* and *D*) except at the tunica vasculosa lentis, a vascular network formed by hyaloid vessels that is regressing at this time via coordinated endothelial apoptosis (85). We also assayed caspase 12 activation because it is specifically localized on the cytoplasmic side of the ER and has been proposed as one of the initiator caspases in UPR-induced death in mice (86). By Western blotting, we found that pro-caspase 12 is cleaved into shorter fragments in transgenics, consistent with the induction of cell death in transgenic lenses (Fig. 12*G*).

The Activation of UPR Sensors Is Also Seen in the Col4a1 Mutants—Because mutations in ECM genes are known to cause cataract, we analyzed the activation of UPR pathways in a cataractous mouse model carrying mutations in an endogenous ECM gene that would let us assess the contribution of UPR activation to cataractogenesis associated with physiological lev-

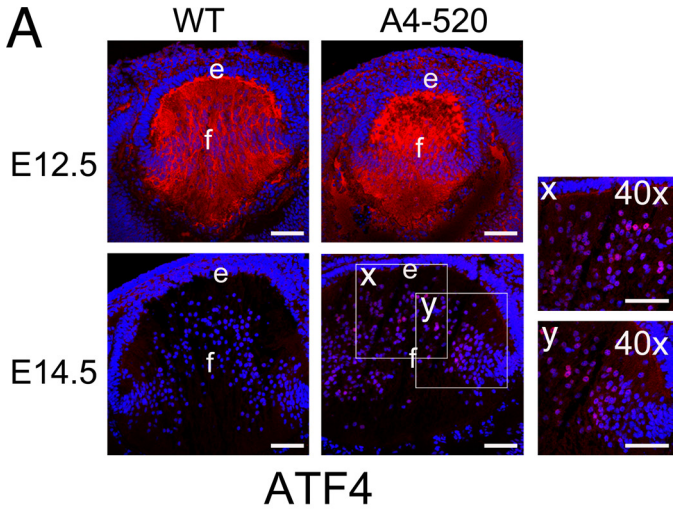

FIGURE 11. **ATF4 and its target CHOP are expressed by the transgenic fiber cells.** *A*, expression of ATF4 (*red*) in WT (*left*) and A4-520 (*right*) lenses detected by immunofluorescence. At E12.5, ATF4 is present in the cytoplasm of both normal and transgenic lenses. However, at E14.5, transgenic fiber cells exhibit elevated levels of nuclear ATF4 in fiber cells. The ×40 magnification images (*40*×) (*x* and *y*) on the *right* show the *boxed regions* from transgenic lenses. *B*, immunoblot analysis of ATF4 and CHOP expression. ATF4 was detected as *two bands*. The *lower band* was abundantly produced in both normal and transgenic lenses, whereas the 50 kDa band (marked with an *asterisk*) was found only in the transgenics. The 29-kDa CHOP (marked with an *asterisk*) was only found in the transgenic lenses. *C*, expression of CHOP (*red*) in WT (*left*) and A4-520 (*right*) lenses detected by immunofluorescence. At E12.5, there is a very weak CHOP expression in transgenic fiber cells. At E14.5, a group of fiber cells express CHOP strongly in their nuclei. The ×40 magnification images (*40*×) (*x* and *y*) on the *right* show the *boxed regions* from transgenic lenses. *Bars*, 77 μm; *e*, epithelium; *f*, fiber cells. In all *panels*, *blue* labels DNA.

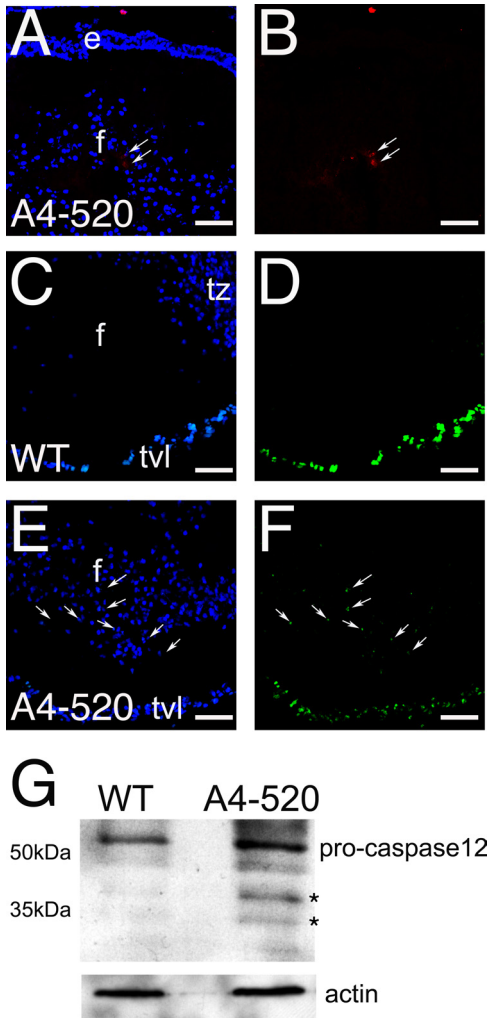

FIGURE 12. **Apoptosis is induced in some transgenic fiber cells at E18.5.** *A* and *B*, cleaved caspase 3 was detected in a group of central fiber cells by immunofluorescence. *A*, an antibody specific to the cleaved form of caspase 3 (*red*) was used to detect the activation of this caspase in E18.5 transgenic lenses. Note the *red staining* in A4-520 transgenic fiber cells indicated with *arrows*. *B*, cleaved caspase 3 staining (*red*) without the nuclear counterstain. *C–E*, apoptotic cells were detected by TUNEL staining. *C*, TUNEL staining (*green*) of E18.5 WT lenses. Note that no WT lens cells are found to be TUNEL-positive, whereas the blood vessels behind the lens (tunica vasculosa lentis) are positively stained. *D*, TUNEL staining (*green*) of WT lenses without the nuclear stain. *E*, TUNEL staining (*green*) of E18.5 A4-520 lenses. A group of central A4-520 fiber cells (indicated by *arrows*) are stained TUNEL-positive. *F*, TUNEL staining (*green*) of A4-520 lenses without the nuclear stain. In all *panels*, *blue* labels DNA. *Bars*, 77 μm. *e*, epithelial cells, *f*, fiber cells; *tvl*, tunica vasculosa lentis. *G*, activation of caspase-12 in E18.5 transgenic lenses examined by Western blot analysis. *Asterisks*, active forms of caspase-12 detected with anti-caspase-12 antibody.

els of mutant protein accumulation. *Col4a1* mutant mice that carry a mutation in exon 40 of *Col4a1* develop porencephaly and cataractous lenses (19, 87). Immunostaining using an antibody specific for COL4A1 showed that the mutant COL4A1 chains are accumulating inside the lens cells. The strongest accumulation was detected in lens epithelial cells (Fig. 13*E*), but some retention was also seen in fiber cells (Fig. 13*G*). Notably, COL4A2 also appeared to be partially retained in lens epithelial cells, indicating co-accumulation with abnormal COL4A1 in the secretory pathway (Fig. 13*H*). We then showed that this accumulation of collagen chains activates UPR pathways but to a much lesser degree when compared with the transgenic mice. Mutant lenses had up-regulation of BiP and ATF6 in both the mutant epithelium and fiber cells (Fig. 14, *A* and *B*). Total XBP1

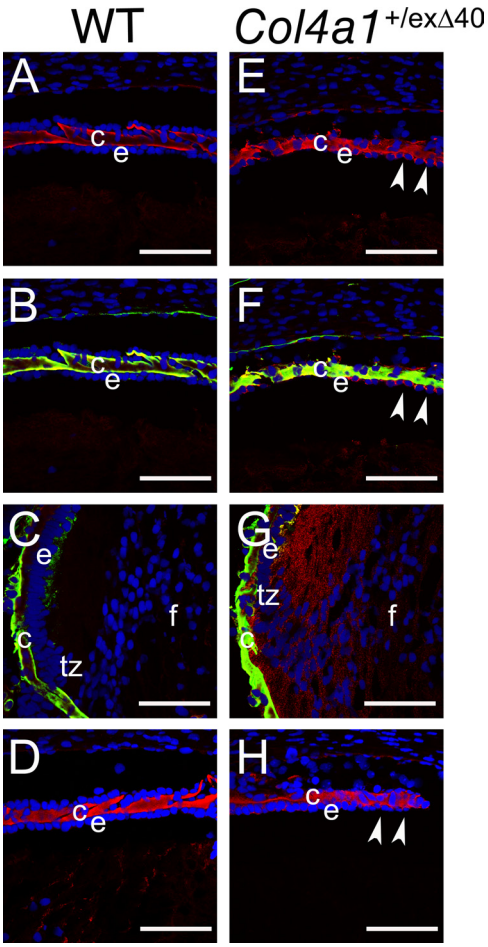

FIGURE 13. **Mutant COL4A1 accumulates in *Col4a1*$^{+/ex\Delta40}$ lenses along with its binding partner COL4A2.** Chain-specific antibodies against COL4A1, laminin, and COL4A2 were used to detect these proteins in WT (*left*) and *Col4a1*$^{+/ex\Delta40}$ lenses (*right*). At E18.5, COL4A1 (*A–C*, *red*), laminin (*B* and *C*, *green*), and COL4A2 (*D*, *red*) are secreted into the lens capsule of normal lenses. In mutant lenses, COL4A1 accumulates inside mutant *Col4a1*$^{+/ex\Delta40}$ lens epithelial (*E* and *F*, *red*) and fiber cells (*G*, *red*). Similarly, COL4A2 also partially accumulates inside mutant lens cells (*H*). The *arrowheads* indicate the epithelial cells that retain collagen chains in mutant lenses. *Bars*, 77 μm. *c*, lens capsule; *e*, epithelium; *f*, fiber cells; *tz*, transition zone. *Blue*, DNA; *red*, collagen chains; *green*, pan-laminin.

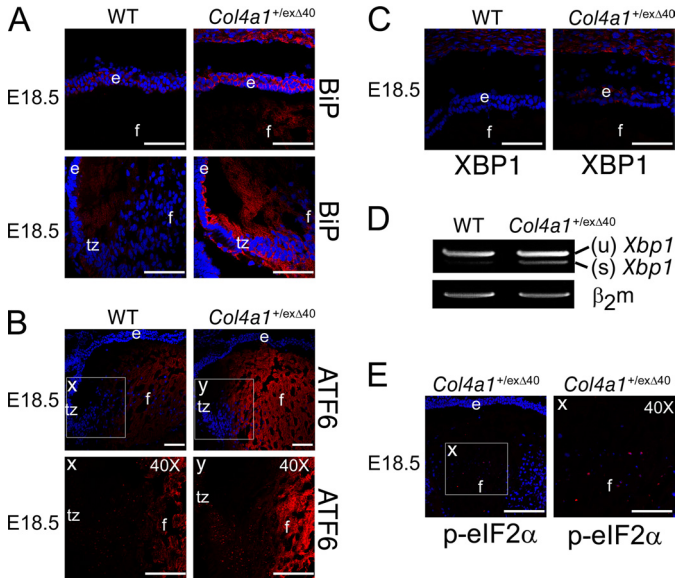

FIGURE 14. **UPR is activated in the *Col4a1*$^{+/ex\Delta40}$ lenses.** *A*, expression of BiP (*red*) in WT (*left*) and *Col4a1*$^{+/ex\Delta40}$ (*right*) lenses detected by immunofluorescence. At E18.5, BiP is up-regulated in mutant lens epithelium and fiber cells. *B*, expression of ATF6 (*red*) in WT (*left*) and *Col4a1*$^{+/ex\Delta40}$ (*right*) lenses detected by immunofluorescence. ATF6 is up-regulated in mutant lens epithelium and fiber cells. The ×40 magnification images (*40*×) (*x* and *y*) at the *bottom panels* show the *boxed regions* from the *top panels*. *C*, expression of XBP1 (*red*) in WT (*left*) and *Col4a1*$^{+/ex\Delta40}$ (*right*) lenses detected by immunofluorescence. XBP1 up-regulation is detected in parts of the epithelium. *D*, RT-PCR analysis of *Xbp1* splicing in WT and *Col4a1*$^{+/ex\Delta40}$ lenses. The splicing of *Xbp1* is induced in the mutant lenses. *E*, expression of phospho-eIF2α (*red*) in *Col4a1*$^{+/ex\Delta40}$ lenses detected by immunofluorescence. Note that phospho-eIF2α is expressed by some central mutant fiber cells at E18.5. The ×40 magnification image (*40*×) (*x*) on the *right* shows the *boxed regions* from *Col4a1*$^{+/ex\Delta40}$ lenses on the *left*. *Bars*, 77 μm; *e*, epithelium; *f*, fiber cells. In all *panels*, *blue* labels DNA.

levels were increased in some parts of the epithelium (Fig. 14*C*), and RT-PCR analysis showed that this *Xbp1* was being spliced in the mutant lenses (Fig. 14*D*). We also detected the presence of phosphorylated eIF2α in a few central fiber cells (Fig. 14*E*). However, the increased nuclear expression of ATF4 or CHOP induction was not detected in the mutant lenses, whereas these lenses were also negative for cleaved caspase 3 staining (data not shown), suggesting that there is no UPR-mediated cell death in these mutant lenses. These results suggest that the accumulation of mutant chains in the secretory pathway at physiological levels can also activate UPR pathways in the lens, and this activation may contribute to the cataract pathogenesis seen in several ECM disorders.

DISCUSSION

It has been previously proposed that UPR can be induced in the lens by oxidative insults, and UPR activation could influence cataractogenesis caused by oxidative stress (41). However, the impact of UPR activation on lens cell fate and/or differentiation programs has not been previously studied *in vivo*. Here we investigated the contribution of UPR induced by unfolded protein accumulation in the ER to cataractogenesis both in an induced transgenic and physiologically relevant disease model. The transgenic lenses studied express elevated levels of normal COL4A3 or COL4A4 chains that cannot assemble alone into heterotrimers and thus accumulate within the secretory pathway (Fig. 2). In contrast, *Col4a1*$^{+/ex\Delta40}$ mice, which have been described as an animal model of hereditary porencephaly, do not efficiently assemble the COL4(A1.A1.A2) heterotrimer, leading to intracellular retention of both COL4A1 and COL4A2 (Fig. 13). We have found that both in transgenic and mutant lenses, the accumulation of collagen chains in the lens secretory pathway activates the unfolded protein response.

In transgenic lenses, this activation interfered with several aspects of lens fiber cell differentiation resulting in distorted fiber cell structure and function (Fig. 15). The differentiation of epithelial cells to fiber cells is a well defined developmental pathway and depends on a highly coordinated set of events, including withdrawal from cell cycle, extensive cell elongation, storage of crystallin proteins, and degradation of nuclei and organelles (51). The altered fiber cells experiencing ER stress, on the other hand, exhibited retention of the nuclei and organelles, defective fiber cell elongation, and reduced crystallin synthesis. The detrimental effects of UPR activation in the

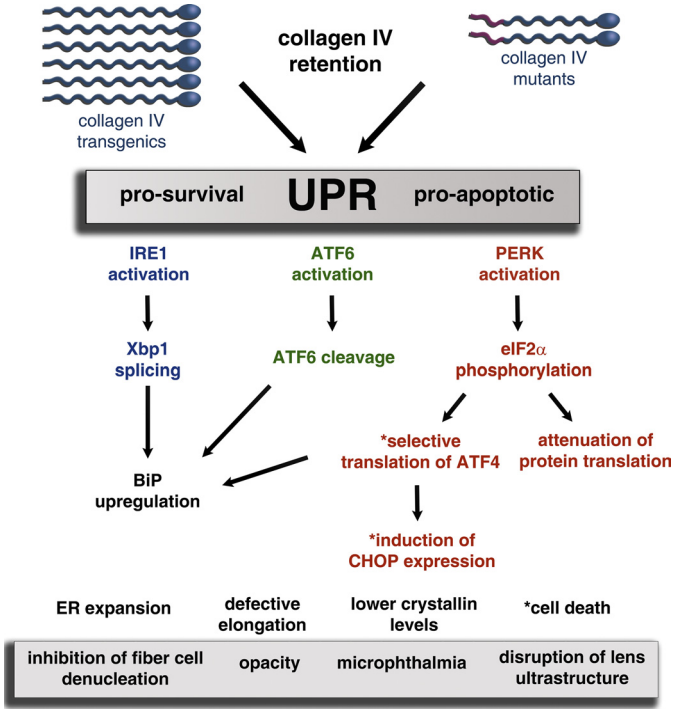

FIGURE 15. **UPR is activated in the lenses of transgenic and mutant mice upon accumulation of collagen chains.** In transgenics, exogenous expression of *Col4a3* or *Col4a4* genes in the embryonic lens causes high levels of collagen chain accumulation inside the transgenic fiber cells and results in immediate activation of all three known UPR sensors. In *Col4a1*$^{+/ex\Delta 40}$ mice, mutant COL4A1 chains cannot properly assemble and accumulate in lens cells along with COL4A2 and activate all three UPR sensors. In transgenics, the translational attenuation induced upon eIF2α phosphorylation negatively affects the synthesis and accumulation of major lens proteins, crystallins. The phosphorylation of eIF2α also results in selective translation of ATF4 and induction of its target CHOP in transgenic lenses, whereas in mutants, this response has not been detected (marked with an *asterisk*). Transgenic lens fiber cells experiencing UPR activation exhibited defective fiber cell elongation around E15.5 and cell death later in E18.5. In contrast, cell death was not observed in mutants (marked with an *asterisk*). Overall, the data suggest that all UPR responses could contribute to the lens pathology observed, including inhibition of denucleation, disruption of lens ultrastructure, opacity, and microphthalmia.

lens were probably mediated by both activation of UPR-specific transcription factors and UPR-induced global translational attenuation. The production of ATF6(N) and XBP1(S) could alter fiber cell transcriptional programs by up-regulating genes involved in ER folding and ER biogenesis in lens fiber cells that would normally undergo programmed degradation of nuclei and cytoplasmic organelles (59, 62, 88). On the other hand, PERK-mediated translational attenuation could interfere with lens fiber cell differentiation through lowering the synthesis of crystallins and other fiber cell-specific proteins that are needed for fiber cell differentiation. The active PERK pathway has been shown to be essential for survival of cells upon ER stress because it aims at decreasing the load on the already challenged ER (79). However, because epithelial to fiber differentiation involves large amounts of protein synthesis, translational attenuation in the lens might cause adverse effects upon differentiation. Notably, a major defect that we observed was in elongation of lens fiber cells during embryogenesis (Fig. 3), which could be related to the insufficient production of fiber cell-specific membrane or other elongation-associated proteins (89). Although fiber cells experiencing UPR showed major structural defects, we did not detect the induction of cell death in the transgenic lens cells prior to E18.5; however, at this time, we detected a group of apoptotic fiber cells in the center of the lens (Fig. 12). This suggests that the induction of cell death is a later response in UPR signaling restricted to a subset of cells that probably experienced prolonged UPR activation because the center of the lens is composed of the oldest fiber cells (90). In contrast, we could not detect cell death in *Col4a1*$^{+/\Delta ex40}$ lenses. Because mutant lenses have lower levels of collagen accumulation in the lens, apoptosis appears to only occur upon severe UPR activation (Fig. 15).

However, the transgenic mouse data propose that early UPR responses, such as translational inhibition, can disrupt the highly coordinated events of fiber cell maturation, leading to defective lens physiology and function. Thus, although the lower activation levels of UPR sensors in *Col4a1*$^{+/\Delta ex40}$ lenses make the contribution of UPR to cataractogenesis less clear in this case, the activation of UPR pathways in the lens could be subtle but still be detrimental to lens structure even without the induction of cell death. Tsang *et al.* (27) showed similar results with transgenic mice expressing mutant collagen X in hypertrophic chondrocytes, where the resulting UPR activation did not induce cell death but altered chondrocyte differentiation and function, causing chondroplasia.

Humans carrying *COL4A1* mutations develop cataracts; however, the underlying mechanism has not been identified (17, 18). In both the human patients and mutant mice, the eye phenotype shows great variations, suggesting the influence of multiple factors (19, 21). However, the absence of a phenotype in mice heterozygous for a null allele of *Col4a1* and *Col4a2* suggests that the mutant protein is required to cause the disease (91). Numerous other ECM disorders also have associated lens defects, but the etiology of the cataracts is largely undetermined. For instance, cataracts and/or lenticonus are reported in Alport syndrome caused by mutations in either COL4A3, COL4A4, or COL4A5 (92), and it has been reported that the lens epithelial cells from cataractous lenses were irregular in shape and had a dilated ER and Golgi consistent with UPR activation (93, 94). Similar to the findings with mice null for *Col4a1* and *Col4a2*, we found that lenses from *Col4a3* null mice are transparent and do not show any gene expression changes by microarray analysis, suggesting that the presence of mutant chains is needed to cause the cataract pathology.[5]

Moreover, the clinical heterogeneity of the cataracts associated with porencephaly and Alport syndrome could be associated with variation in the extent of UPR activation, because the level of UPR activation is directly related to the strength and/or duration of the ER stress experienced, and it may vary between different individuals, leading to different clinical outcomes. Thus, the possibility that the activation of UPR pathways upon the accumulation of mutant collagen chains within the ER contributes to the cataract pathology in these disorders is an attractive theory. However the evidence for a direct role of UPR in the cataracts seen in humans and mice harboring mutations in collagen genes is still missing, and further research is needed to reveal a better understanding of the role of UPR in lens

[5] B. P. Danysh and M. K. Duncan, unpublished data.

pathology. Nevertheless, our results support the proposition that UPR can be a common cataractogenic mechanism in disorders resulting from abnormal ECM molecule production by the lens.

Acknowledgments—We thank Lixing Reneker (University of Missouri School of Medicine, Columbia, MO) for providing the δEN/αA-crystallin promoter, Yoshikazu Sado (Shigei Medical Research Institute, Okayama, Japan) for the chain-specific collagen IV antibodies, Samuel Zigler (The Johns Hopkins University School of Medicine, Baltimore, MD) for the crystallin antibodies, and Dave Scheiblin (University of Delaware, Newark, DE) for technical support with scanning electron microscopy.

REFERENCES

1. Brian, G., and Taylor, H. (2001) *Bull. World Health Organ.* **79,** 249–256
2. Thylefors, B., Négrel, A. D., Pararajasegaram, R., and Dadzie, K. Y. (1995) *Bull. World Health Organ.* **73,** 115–121
3. Moore, A. T. (2004) *Br. J. Ophthalmol.* **88,** 2–3
4. Francis, P. J., Berry, V., Bhattacharya, S. S., and Moore, A. T. (2000) *J. Med. Genet.* **37,** 481–488
5. Congdon, N., Vingerling, J. R., Klein, B. E., West, S., Friedman, D. S., Kempen, J., O'Colmain, B., Wu, S. Y., and Taylor, H. R. (2004) *Arch. Ophthalmol.* **122,** 487–494
6. Ellwein, L. B., and Urato, C. J. (2002) *Arch. Ophthalmol.* **120,** 804–811
7. Hutnik, C. M., and Nichols, B. D. (1999) *Curr. Opin. Ophthalmol.* **10,** 22–28
8. Shiels, A., and Hejtmancik, J. F. (2007) *Arch. Ophthalmol.* **125,** 165–173
9. Spierer, A., Desatnik, H., Rosner, M., and Blumenthal, M. (1998) *J. Pediatr. Ophthalmol. Strabismus* **35,** 281–285
10. Seery, C. M., Pruett, R. C., Liberfarb, R. M., and Cohen, B. Z. (1990) *Am. J. Ophthalmol.* **110,** 143–148
11. Snead, M. P., and Yates, J. R. (1999) *J. Med. Genet.* **36,** 353–359
12. Colville, D. J., and Savige, J. (1997) *Ophthalmic Genet.* **18,** 161–173
13. Junk, A. K., Stefani, F. H., and Ludwig, K. (2000) *Arch. Ophthalmol.* **118,** 895–897
14. Kato, T., Watanabe, Y., Nakayasu, K., Kanai, A., and Yajima, Y. (1998) *Jpn. J. Ophthalmol.* **42,** 401–405
15. Breedveld, G., de Coo, I. F., Lequin, M. H., Arts, W. F., Heutink, P., Gould, D. B., John, S. W., Oostra, B., and Mancini, G. M. (2006) *J. Med. Genet.* **43,** 490–495
16. Sibon, I., Coupry, I., Menegon, P., Bouchet, J. P., Gorry, P., Burgelin, I., Calvas, P., Orignac, I., Dousset, V., Lacombe, D., Orgogozo, J. M., Arveiler, B., and Goizet, C. (2007) *Ann. Neurol.* **62,** 177–184
17. Vahedi, K., Kubis, N., Boukobza, M., Arnoult, M., Massin, P., Tournier-Lasserve, E., and Bousser, M. G. (2007) *Stroke* **38,** 1461–1464
18. van der Knaap, M. S., Smit, L. M., Barkhof, F., Pijnenburg, Y. A., Zweegman, S., Niessen, H. W., Imhof, S., and Heutink, P. (2006) *Ann. Neurol.* **59,** 504–511
19. Gould, D. B., Phalan, F. C., Breedveld, G. J., van Mil, S. E., Smith, R. S., Schimenti, J. C., Aguglia, U., van der Knaap, M. S., Heutink, P., and John, S. W. (2005) *Science* **308,** 1167–1171
20. Favor, J., Gloeckner, C. J., Janik, D., Klempt, M., Neuhäuser-Klaus, A., Pretsch, W., Schmahl, W., and Quintanilla-Fend, L. (2007) *Genetics* **175,** 725–736
21. Van Agtmael, T., Schlötzer-Schrehardt, U., McKie, L., Brownstein, D. G., Lee, A. W., Cross, S. H., Sado, Y., Mullins, J. J., Pöschl, E., and Jackson, I. J. (2005) *Hum. Mol. Genet.* **14,** 3161–3168
22. de Almeida, S. F., Fleming, J. V., Azevedo, J. E., Carmo-Fonseca, M., and de Sousa, M. (2007) *J. Immunol.* **178,** 3612–3619
23. Baryshev, M., Sargsyan, E., Wallin, G., Lejnieks, A., Furudate, S., Hishinuma, A., and Mkrtchian, S. (2004) *J. Mol. Endocrinol.* **32,** 903–920
24. Schröder, M., and Kaufman, R. J. (2005) *Mutat. Res.* **569,** 29–63
25. Southwood, C. M., Garbern, J., Jiang, W., and Gow, A. (2002) *Neuron* **36,** 585–596
26. Thomas, M., Yu, Z., Dadgar, N., Varambally, S., Yu, J., Chinnaiyan, A. M., and Lieberman, A. P. (2005) *J. Biol. Chem.* **280,** 21264–21271
27. Tsang, K. Y., Chan, D., Cheslett, D., Chan, W. C., So, C. L., Melhado, I. G., Chan, T. W., Kwan, K. M., Hunziker, E. B., Yamada, Y., Bateman, J. F., Cheung, K. M., and Cheah, K. S. (2007) *PLoS Biol.* **5,** e44
28. Wilson, R., Freddi, S., Chan, D., Cheah, K. S., and Bateman, J. F. (2005) *J. Biol. Chem.* **280,** 15544–15552
29. Yoshida, H. (2007) *FEBS J.* **274,** 630–658
30. Gow, A., and Sharma, R. (2003) *Neuromolecular Med.* **4,** 73–94
31. Harding, H. P., and Ron, D. (2002) *Diabetes* **51,** Suppl. 3, S455–S461
32. Imaizumi, K., Miyoshi, K., Katayama, T., Yoneda, T., Taniguchi, M., Kudo, T., and Tohyama, M. (2001) *Biochim. Biophys. Acta* **1536,** 85–96
33. Lindholm, D., Wootz, H., and Korhonen, L. (2006) *Cell Death Differ.* **13,** 385–392
34. Harding, H. P., Calfon, M., Urano, F., Novoa, I., and Ron, D. (2002) *Annu. Rev. Cell Dev. Biol.* **18,** 575–599
35. Zhang, K., and Kaufman, R. J. (2004) *J. Biol. Chem.* **279,** 25935–25938
36. Knowlton, A. A. (2007) *Cardiovasc. Res.* **73,** 1–2
37. Szegezdi, E., Logue, S. E., Gorman, A. M., and Samali, A. (2006) *EMBO Rep.* **7,** 880–885
38. Xu, C., Bailly-Maitre, B., and Reed, J. C. (2005) *J. Clin. Invest.* **115,** 2656–2664
39. Brewer, J. W., and Diehl, J. A. (2000) *Proc. Natl. Acad. Sci. U.S.A.* **97,** 12625–12630
40. Iwakoshi, N. N., Lee, A. H., Vallabhajosyula, P., Otipoby, K. L., Rajewsky, K., and Glimcher, L. H. (2003) *Nat. Immunol.* **4,** 321–329
41. Mulhern, M. L., Madson, C. J., Danford, A., Ikesugi, K., Kador, P. F., and Shinohara, T. (2006) *Invest. Ophthalmol. Vis. Sci.* **47,** 3951–3959
42. Ikesugi, K., Yamamoto, R., Mulhern, M. L., and Shinohara, T. (2006) *Exp. Eye. Res.* **83,** 508–516
43. Reneker, L. W., Chen, Q., Bloch, A., Xie, L., Schuster, G., and Overbeek, P. A. (2004) *Invest. Ophthalmol. Vis. Sci.* **45,** 4083–4090
44. Kobayashi, T., and Uchiyama, M. (2003) *Kidney Int.* **64,** 1986–1996
45. Duncan, M. K., Xie, L., David, L. L., Robinson, M. L., Taube, J. R., Cui, W., and Reneker, L. W. (2004) *Invest. Ophthalmol. Vis. Sci.* **45,** 3589–3598
46. Duncan, M. K., Cvekl, A., Li, X., and Piatigorsky, J. (2000) *Invest. Ophthalmol. Vis. Sci.* **41,** 464–473
47. Reed, N. A., Oh, D. J., Czymmek, K. J., and Duncan, M. K. (2001) *J. Immunol. Methods* **253,** 243–252
48. Garadi, R., Foltyn, A. R., Giblin, F. J., and Reddy, V. N. (1984) *Invest. Ophthalmol. Vis. Sci.* **25,** 147–152
49. Opdenaker, L. M., and Farach-Carson, M. C. (2009) *J Cell Biochem.* **107,** 473–481
50. Kelley, P. B., Sado, Y., and Duncan, M. K. (2002) *Matrix Biol.* **21,** 415–423
51. Piatigorsky, J. (1981) *Differentiation* **19,** 134–153
52. Lovicu, F. J., and Robinson, M. L. (2004) *Development of the Ocular Lens*, pp. 214–225, Cambridge University Press, Cambridge
53. Fuhrmann, C., and Bereiter-Hahn, J. (1984) *Histochemistry* **80,** 153–156
54. Kuemmel, T. A., Thiele, J., Hafenrichter, E. G., Varus, E., and Fischer, R. (1996) *J. Submicrosc. Cytol. Pathol.* **28,** 537–551
55. Kaufman, R. J. (1999) *Genes Dev.* **13,** 1211–1233
56. Kaufman, R. J. (2002) *J. Clin. Invest.* **110,** 1389–1398
57. Lee, A. S. (2005) *Methods* **35,** 373–381
58. Bertolotti, A., Zhang, Y., Hendershot, L. M., Harding, H. P., and Ron, D. (2000) *Nat. Cell Biol.* **2,** 326–332
59. Sriburi, R., Jackowski, S., Mori, K., and Brewer, J. W. (2004) *J. Cell Biol.* **167,** 35–41
60. Lee, A. H., Chu, G. C., Iwakoshi, N. N., and Glimcher, L. H. (2005) *EMBO J.* **24,** 4368–4380
61. Ron, D., and Hampton, R. Y. (2004) *J. Cell Biol.* **167,** 23–25
62. Bommiasamy, H., Back, S. H., Fagone, P., Lee, K., Meshinchi, S., Vink, E., Sriburi, R., Frank, M., Jackowski, S., Kaufman, R. J., and Brewer, J. W. (2009) *J. Cell Sci.* **122,** 1626–1636
63. Schröder, M., and Kaufman, R. J. (2006) *Curr. Mol. Med.* **6,** 5–36
64. Calfon, M., Zeng, H., Urano, F., Till, J. H., Hubbard, S. R., Harding, H. P., Clark, S. G., and Ron, D. (2002) *Nature* **415,** 92–96
65. Lee, K., Tirasophon, W., Shen, X., Michalak, M., Prywes, R., Okada, T., Yoshida, H., Mori, K., and Kaufman, R. J. (2002) *Genes Dev.* **16,** 452–466

66. Yoshida, H., Matsui, T., Yamamoto, A., Okada, T., and Mori, K. (2001) *Cell* **107,** 881–891
67. Yoshida, H., Oku, M., Suzuki, M., and Mori, K. (2006) *J. Cell Biol.* **172,** 565–575
68. Haze, K., Yoshida, H., Yanagi, H., Yura, T., and Mori, K. (1999) *Mol. Biol. Cell* **10,** 3787–3799
69. Shen, J., Chen, X., Hendershot, L., and Prywes, R. (2002) *Dev. Cell* **3,** 99–111
70. Ye, J., Rawson, R. B., Komuro, R., Chen, X., Davé, U. P., Prywes, R., Brown, M. S., and Goldstein, J. L. (2000) *Mol. Cell* **6,** 1355–1364
71. Hong, M., Luo, S., Baumeister, P., Huang, J. M., Gogia, R. K., Li, M., and Lee, A. S. (2004) *J. Biol. Chem.* **279,** 11354–11363
72. Brostrom, C. O., and Brostrom, M. A. (1998) *Prog. Nucleic Acid. Res. Mol. Biol.* **58,** 79–125
73. Ron, D. (2002) *J. Clin. Invest.* **110,** 1383–1388
74. Kaufman, R. J. (2004) *Trends Biochem. Sci.* **29,** 152–158
75. Papaconstantinou, J. (1967) *Science* **156,** 338–346
76. Zigman, S. (1985) *Biol. Bull.* **168,** 189–213
77. Piatigorsky, J. (1992) *J. Biol. Chem.* **267,** 4277–4280
78. Wang, X., Garcia, C. M., Shui, Y. B., and Beebe, D. C. (2004) *Invest. Ophthalmol. Vis. Sci.* **45,** 3608–3619
79. Harding, H. P., Zhang, Y., Bertolotti, A., Zeng, H., and Ron, D. (2000) *Mol. Cell* **5,** 897–904
80. Harding, H. P., Novoa, I., Zhang, Y., Zeng, H., Wek, R., Schapira, M., and Ron, D. (2000) *Mol. Cell* **6,** 1099–1108
81. Ameri, K., Lewis, C. E., Raida, M., Sowter, H., Hai, T., and Harris, A. L. (2004) *Blood* **103,** 1876–1882
82. Ma, Y., Brewer, J. W., Diehl, J. A., and Hendershot, L. M. (2002) *J. Mol. Biol.* **318,** 1351–1365
83. Wang, X. Z., Lawson, B., Brewer, J. W., Zinszner, H., Sanjay, A., Mi, L. J., Boorstein, R., Kreibich, G., Hendershot, L. M., and Ron, D. (1996) *Mol. Cell. Biol.* **16,** 4273–4280
84. Kouroku, Y., Fujita, E., Tanida, I., Ueno, T., Isoai, A., Kumagai, H., Ogawa, S., Kaufman, R. J., Kominami, E., and Momoi, T. (2007) *Cell Death Differ.* **14,** 230–239
85. Mitchell, C. A., Risau, W., and Drexler, H. C. (1998) *Dev. Dyn.* **213,** 322–333
86. Szegezdi, E., Fitzgerald, U., and Samali, A. (2003) *Ann. N.Y. Acad. Sci.* **1010,** 186–194
87. Gould, D. B., Marchant, J. K., Savinova, O. V., Smith, R. S., and John, S. W. (2007) *Hum. Mol. Genet.* **16,** 798–807
88. Sriburi, R., Bommiasamy, H., Buldak, G. L., Robbins, G. R., Frank, M., Jackowski, S., and Brewer, J. W. (2007) *J. Biol. Chem.* **282,** 7024–7034
89. Piatigorsky, J., Webster Hde, F., and Wollberg, M. (1972) *J. Cell Biol.* **55,** 82–92
90. Kuszak, J. R., Zoltoski, R. K., and Sivertson, C. (2004) *Exp. Eye. Res.* **78,** 673–687
91. Pöschl, E., Schlötzer-Schrehardt, U., Brachvogel, B., Saito, K., Ninomiya, Y., and Mayer, U. (2004) *Development* **131,** 1619–1628
92. Wilson, M. E., Jr., Trivedi, R. H., Biber, J. M., and Golub, R. (2006) *J. AAPOS* **10,** 182–183
93. Choi, J., Na, K., Bae, S., and Roh, G. (2005) *Korean J. Ophthalmol.* **19,** 84–89
94. Sargon, M. F., Celik, H. H., and Sener, C. (1999) *Ophthalmologica* **213,** 30–33
95. Rauschert, N., Brändlein, S., Holzinger, E., Hensel, F., Müller-Hermelink, H. K., and Vollmers, H. P. (2008) *Lab. Invest.* **88,** 375–386